

Prognostic Significance and Immune Infiltration of Microenvironment-related Signatures in Pancreatic Cancer

Qian Lu

Tongzhou people's hospital <https://orcid.org/0000-0001-6395-693X>

Yu Zhang

Affiliated Hospital of Nantong University

Weihong Gu

Tongzhou people's hospital

Xinrong Ji

Tongzhou people's hospital

Zhong Chen (✉ chenz19630704@126.com)

Department of General surgery, Affiliated Hospital of Nantong University, Nantong, 226001, China

Primary research

Keywords: Prognostic significance, Immune infiltration, Microenvironment, Biomarkers, Pancreatic Cancer

Posted Date: August 21st, 2020

DOI: <https://doi.org/10.21203/rs.3.rs-60885/v1>

License:  This work is licensed under a Creative Commons Attribution 4.0 International License.

[Read Full License](#)

Version of Record: A version of this preprint was published at Medicine on March 26th, 2021. See the published version at <https://doi.org/10.1097/MD.0000000000024957>.

Abstract

Background: Pancreatic ductal adenocarcinoma (PDAC) is one of the highly fatal and most aggressive types of malignancies and accounts for the vast majority of Pancreatic Cancer (PC). Numerous studies have reported that the tumor microenvironment (TME) was significantly correlated with the oncogenesis, progress, and prognosis of various malignancies. Therefore, mining of TME-related genes is reasonably important to improve the overall survival (OS) of patients with PDAC.

Methods: The Estimation of STromal and Immune cells in MAlignant Tumor tissues using Expression data (ESTIMATE) algorithm was applied to identify differential expressed genes (DEGs). Functional and pathway enrichment analyses, protein–protein interaction (PPI) network construction and module analysis, overall survival analysis and tumor immune estimation resource (TIMER) database analysis were then performed on DEGs.

Results: Data analysis indicated that higher immune scores were correlated with better overall survival ($P = 0.033$). Differential expression analysis obtained 90 intersection genes influencing both stromal and immune scores. Among these intersection genes, CA9, EBI3, SPOCK2, WDFY4, CD1D and CCL22 were significantly correlated with OS in PDAC patients. Moreover, multivariate Cox analysis revealed that CA9, SPOCK2 and CD1D were the most significant prognostic genes, and were closely correlated with immune infiltration in TCGA cohort. Further analysis indicated that CD1D were significantly related with immune cell biomarkers for PDAC patients.

Conclusions: In summary, our findings provide a more comprehensive insight into TME and show a list of prognostic immune associated genes in PDAC. However, further studies on these genes need to be performed to gain additional understanding of the association between TME and prognosis in PDAC.

Background

Pancreatic cancer (PC) is one of the highly fatal and most aggressive types of human malignant tumors worldwide. In 2018, PC was newly diagnosed in ~458 million people and approximately 432 million people died of PC in the whole world—ranking seventh among all cancer-associated mortalities^[1]. Pancreatic ductal adenocarcinoma (PDAC) is an epithelial malignancy which originates from the ductal epithelium of pancreas and accounts for 90% of all cases of PC^[2]. Due to a lack of distinct symptoms, PDAC has often already extensively metastasized at the time of diagnosis—and radical resection is almost impossible^[3, 4]. In spite of extensive efforts over the past few years—the conventional therapies for advanced PDAC, including chemotherapy, radiotherapy and targeted therapies—continues to have the poorest outcome among all the malignancies and the median overall survival (OS) remains approximately six months^[5-7]. Thus, it becomes necessary to identify early diagnostic biomarkers and therapeutic targets of PDAC.

The tumor microenvironment (TME) is a complex and synergistic mixture comprised of fluids, immune cells, stromal cells, extracellular matrix molecules, inflammatory mediators and chemokines. The various constituents of the TME play significant roles in the tumor immune escape, tumor proliferation and metastasis, and it has been shown to be related with diagnosis and clinical outcomes^[8, 9]. Numerous clinical trials of targeting TME showed encouraging results^[10, 11]. Thus, exploring the molecular function and composition of TME is significant to effectively intervene tumor progression and immune response.

Estimation of Stromal and Immune cells in Malignant Tumor tissues using Expression data (ESTIMATE) was created to evaluate tumor purity based on the molecular biomarker expression of stromal and immune cells. The ESTIMATE algorithm has been used to breast cancer^[12], prostate cancer^[13], colorectal cancer^[14], and other studies about tumor microenvironment^[15]. However, prognostic value of ESTIMATE algorithm in PDAC is still unclear. In the present study, we applied the ESTIMATE algorithm to identify prognostic biomarkers and explore the immune infiltration of prognostic genes in PDAC.

Materials And Methods

Data Source

Immune scores and stromal scores of PDAC patients were obtained from ESTIMATE (<http://bioinformatics.mdanderson.org/estimate/>) designed by Yoshihara et al^[16]. Gene expression profile (level 3 data) and clinical information for PDAC patients was collected from the TCGA data portal (<https://tcga-data.nci.nih.gov/tcga/>). Only samples in accordance with the following inclusion criteria in the present study: (a) available immune and stromal scores; (b) available gene expression information; (c) the overall survival (OS) days ≥ 30 days.

Identification and Functional enrichment analyses of DEGs

X-tile software was used to identify cutoff criteria for the ESTIMATE scores, immune score and stromal score. According to the cutoff point, we stratify PDAC patients into low-score and high-score subgroups. Data analysis was performed by use of package limma^[17] in R software (version 3.6.0). The threshold of DEGs were: $|\log_2 \text{fold change} (\log_2 \text{FC})| > 1.5$ and false discovery rate (FDR) < 0.05 . DAVID (<http://david.ncifcrf.gov>, Version 6.8) online analysis tool was undertaken to assess the role of intersection genes in PDAC. P-value < 0.05 was considered to be statistically significant. The Gene Ontology (GO) analysis shows the DEG function at the level of three main categories (molecular function, biological process and cellular component), and the KEGG analysis reveals the pathway enrichment of DEGs.

Construction of Protein-Protein Interaction (PPI) Network

The PPI network of DEGs was constructed using retrieved through the Search Tool for the Retrieval of Interacting Genes (STRING, <https://string-db.org/>)^[18] and Cytoscape software (version 3.5)^[19] were used for the reconstruction of the PPI network. The Molecular Complex Detection (MCODE) (version 1.4.2)

plugin of Cytoscape was applied to identify the most significant module based upon topology to locate densely connected regions. The selection criteria were as follows: maximum depth = 100, degree cut-off = 2, node score cut-off = 0.2, and k-core = 2.

Overall Survival Analysis

The relationship between the OS of PDAC patients and the expression of DEGs was illustrated by Kaplan-Meier plots using R. Kaplan-Meier plotter (<http://kmplot.com/analysis/>) online analysis tool was applied to verify the prognostic value of survival related DEGs. The relationship was determined by log-rank test. P-value < 0.05 was considered to be statistically significant.

TIMER database analysis

We analyzed comprehensive correlation between prognostic genes expression and tumor-infiltrating immune cells gene markers via Tumor Immune Estimation Resource (TIMER, <https://cistrome.shinyapps.io/timer/>). Moreover, the association between somatic copy number alterations (SCNAs) of prognostic genes and immune cell enrichments in PDAC was also analyzed by TIMER.

Results

Relationship between immune/ stromal / ESTIMATE scores and T stage, N stage or M stage

Among the 140 PDAC patients enrolled in the present study, 65 were female and 75 were male. Calculated by the ESTIMATE algorithm, the immune scores ranged from -1559.87 to 2648.04 while the stromal scores from -1843.32 to 2138.93, and ESTIMATE scores ranged from -3187.36 to 4161.76. The distributions of immune, stromal, and ESTIMATE scores did not associate with T stage (Figure 1A–1C), N stage (Figure 1D–1F), or M stage (Figure 1G–1I).

Elevated immune scores associated with a better prognosis

According to immune, stromal, and ESTIMATE scores, 140 PDAC patients were divided into low and high score groups to detect potential relationship between immune/stromal/Estimate score and prognosis. For immune scores, the low score group contained 57 patients, while the high score group contained 83 patients. Kaplan-Meier survival curves showed that elevated immune scores associated with better overall survival (P = 0.033) (Figure 2A). By contrast, stromal scores (P = 0.656) and ESTIMATE scores (P = 0.496) were not correlated with overall survival (Figure 2B, 2C).

Differential expressed genes with immune and stromal score in PDAC

We examined transcriptional microarray data of 140 PDAC cases to identify DEGs with immune and/or stromal scores. Figure 3A and 3B show Volcano plot of gene expression profile in high vs low immune scores groups and stromal scores. Figure 3C shows a heat map of 324 DEGs with high or low immune scores, and Figure 3D shows a heat map of 318 DEGs with high or low stromal scores. According to

immune score comparison, 320 genes were up-regulated and 4 genes down-regulated in the high score than the low score group. For high stromal score group compared with low score group, 297 up-regulated genes and 21 down-regulated genes were detected. A total of 86 DEGs were synchronously upregulated (Figure 3E) in the high stromal score and high immune score groups, and 4 genes were commonly downregulated (Figure 3F) using Venn algorithm.

Functional and pathway enrichment analyses of DEGs

GO and KEGG enrichment analyses were performed to explore the biological classification of DEGs via DAVID online tool. GO analysis results indicated that biological processes (BP) of DEGs were mainly enriched in lymphocyte proliferation, mononuclear cell proliferation, regulation of lymphocyte proliferation (Table 1). Changes in cell component (CC) of DEGs were significantly enriched in immunological synapse, T cell receptor complex, ficolin-1-rich granule membrane (Table 1). Changes in molecular function (MF) of DEGs were mainly enriched in the CD4 receptor binding, MHC protein complex binding and sialic acid binding (Table 1). KEGG pathway analysis showed that the DEGs were significantly enriched in PPAR signaling pathway, Hematopoietic cell lineage and IL-17 signaling pathway (Table 1).

PPI network construction and module analysis

We used Cytoscape to construct the PPI network of intersection DEGs (Figure 4A) and obtain the most significant module (Figure 4B-C). This network composed of four modules, the top two significant modules were selected for further analysis. These modules were named as Modules B, and C, respectively. In Module B, 13 nodes with 35 edges were formed in the network, including ITGAM, GZMA, HCST, CCL17, CD19, CD74, CCL4, TCL1A, CD83, TNFRSF1B, CD22, CD69, MS4A1 (Figure 4B). Module C contained 13 edges involving 7 nodes: SPN, ZAP70, IL2RB, CD1C, KLRB1, ITGAX, BTK (Figure 4C).

Survival analysis of significant DEGs in PDAC

To explore the relationship between commonly DEGs and overall survival, we performed Kaplan-Meier survival curves by using the TCGA database. The Kaplan-Meier results indicated that decreased CA9, MUC5AC, P2RY8 mRNA expression significantly associated with poor OS ($p < 0.05$), and elevated CD36, EBI3, PLA2G2D, SPOCK2, WDFY4, CD1D, CCL22 mRNA expression was significantly correlated with shorter OS for PDAC patients ($P < 0.05$) (Figure 5). Then, we validate the prognostic value of survival related DEGs using Kaplan-Meier plotter online analysis tool. The results show CA9, EBI3, SPOCK2, WDFY4, CD1D, CCL22 mRNA expression was significantly correlated with OS ($P < 0.05$) (Figure 6).

Univariate and multivariate Cox logistic regression analysis of overall survival

As shown in Table 2, EBI3, P2RY8, CA9, CD36, SPOCK2, CCL22, CD1D expression (ref. low), T stage (ref. T1-T4) and N stage (ref. N0-1) were demonstrated as independent prognostic indicators for PDAC patients ($p < 0.05$). Multivariate Cox analysis revealed that poor OS was significantly associated with CA9 expression (ref. low; HR=2.751, $p=0.008$), SPOCK2 expression (ref. low; HR=3.310, $p=0.016$), CD1D expression (ref. low; HR=0.212, $p=0.034$) and N stage (ref. N0-1; HR=2.849, $p=0.029$).

Immune infiltration of CA9, SPOCK2 and CD1D

After validating prognostic value of CA9, SPOCK2 and CD1D, we performed correlation analysis between CA9, SPOCK2 and CD1D and immune infiltration level for PDAC in Figure 7. Scatter plots were generated with partial Spearman's correlation and statistical significance. CD1D expression were significantly associated purity (correlation=-0.283). In addition, SPOCK2 and CD1D significantly associated with B cell, CD8+ T cell, CD4+ T cell, macrophage, neutrophil, and dendritic cell infiltration, CA9 significantly associated with CD8+ T cell, macrophage, neutrophil, and dendritic cell infiltration ($p < 0.05$). To further explore the association between genomic metrics of CA9, SPOCK2 and CD1D and the immune cell enrichment, PDAC with SCNAs were divided into four levels, including arm-level deletion, diploid/normal, arm-level gain, and high amplification. We examined infiltration of six immune cell types, including B cell, CD8+T cell, CD4+T cell, macrophage cell, neutrophil cell, and dendritic cell. The results showed that the extent of immune infiltration was largely different in PDAC with different SCNAs of CA9, SPOCK2 and CD1D (Figure 8). Enrichment of B cell, CD4+T cell displayed significant downregulation in PDAC with particular SCNA of CA9. In addition, decreasing of B cell, CD8+T cell, CD4+T cell, macrophage cell and neutrophil cell enrichments was also detected in PDAC with particular SCNA of SPOCK2 and CD1D. Therefore, the results revealed that genomic alterations of CA9, SPOCK2 and CD1D were associated with the extent of immune infiltration in PDAC.

Discussion

PDAC is one of the highly fatal and most aggressive types of malignancies and approximately accounts for 90% of all cases of PC^[2]. Numerous studies have reported that the tumor microenvironment (TME) was significantly correlated with the oncogenesis, progress, and prognosis of various malignancies^[20-22]. The Interplay between tumor cells and the Immune System in TME reflect the plasticity of immune system and the tumor^[23]. Tumor development is closely related to TME, and any changes of the component of TME may affect the progression of malignancies^[23]. Exploring the alterations may help the advance of therapeutic strategies. Immune cells and stromal cells are the important compositions of TME, which play a key role in the progress of cancers^[24]. The ESTIMATE algorithm based on gene expression profile has been applied for the exploration of breast cancer, prostate cancer, colorectal cancer and shown good clinical application value^[12-14]. However, it has not been used for the investigation of PDAC.

In the present work, we used ESTIMATE algorithm to calculate immune scores, which indicate the intensity of immune cells infiltration in tumor^[16]. Our result indicated that high immune score was related with improved OS. Recent researches have similar findings. Heeren et al^[25] found that the number of CD4(+) T-cell is significantly higher in lymph node-negative samples than in lymph node- positive ones. Moreover, Punt et al^[26] reported that TCL1A expression of B cell associated with better survival in Cervical cancer. These results may suggest that immune cells infiltrating tumor tissue affect tumor progression. In order to explore the potential TME related gene in PDAC, we performed bioinformation analysis to identify

intersection DEGs in both stromal and immune cells. Finally, 86 upregulated commonly genes and 4 downregulated commonly genes were obtained between the stromal and immune score groups. These 90 intersection genes were correlated with biological processes in the TME, including lymphocyte proliferation, mononuclear cell proliferation, regulation of lymphocyte proliferation. These processes may play a significant role in tumor development and metastasis and significantly influence OS^[27]. Among molecular functions, intersection genes enriched in the CD4 receptor binding, MHC protein complex binding and sialic acid binding. CD4+ T cells constitute an important component of tumor infiltrating lymphocytes and exert a key role in tumor immune-surveillance^[28]. Moreover, it has been demonstrated that interactions with sialic acid-binding receptors can significantly affect cancer progression^[29].

Next, we performed Kaplan-Meier survival curves to detect prognostic immune associated genes in PDAC and validate by Kaplan-Meier plotter online analysis tool. The results indicated that CA9, EBI3, SPOCK2, WDFY4, CD1D and CCL22 were significantly correlated with OS in patients with PDAC. Of the 6 genes identified, CA9^[30], EBI3^[31] have been proved to be involved in PDAC progression or significant in predicting OS, suggesting that our bioinformation analysis based on TCGA has prognostic values. The remaining 4 genes include SPOCK2, WDFY4, CD1D, CCL22 have not or rarely been reported in PDAC prognosis previously, and may become potential biomarkers for PDAC.

Subsequently, the expression of CA9, EBI3, SPOCK2, WDFY4, CD1D and CCL22 were enrolled in multivariate analysis for OS in PDAC. Importantly, CA9 and SPOCK2 and CD1D were demonstrated as independent prognostic indicators for PDAC patients. CA9, Carbonic anhydrase 9, is a cancer-related cell surface enzyme catalyzing the reversible conversion of carbon dioxide to bicarbonate ion and proton^[32]. Cells will accelerate metabolism and produce excess acid in a hypoxic microenvironment, which activates the catalytic activity of CA9 to regulate the intracellular and extracellular pH perturbations^[33]. Moreover, CA9 expressed in many tumor types also plays an important role in cell adhesion and spreading^[34]. Therefore, in hypoxia or acidosis environments, CA9 can raise the survival advantage of tumor cells and enhance their ability of migration, invasion and metastasis^[35]. A recent research showed that in response to hypoxia, PDAC cells expressing activated KRAS increase expression of CA9, via stabilization of HIF1A and HIF2A, to regulate pH and glycolysis^[30]. Combined with our analysis, it highlights the possibility of CA9 as a targeted therapy for PDAC. The full name of SPOCK2 is SPARC (osteonectin), cwcvc and kazal-like domains proteoglycan 2, which is a glycoprotein composed of a protein domain, 2 chondroitin side chains, and heparan sulfate^[36]. A recent study showed that hypermethylation of the SPOCK2 in colon cancer is significantly higher than in normal mucosal tissues adjacent to the cancer^[37]. In addition, Ren F et al revealed that hypermethylation of SPOCK2 is associated with endometriosis-related ovarian endometrioid adenocarcinoma^[38] and that SPOCK2 regulates biological behavior of endometrial cancer cells through regulating the protein expression of MT1-MMP and MMP2 and the activation of MMP2^[39]. These evidences indicated that the abnormality of SPOCK2 may contribute to tumorigenesis and the progression of tumors. However, the role of the SPOCK2 has not been researched in PDAC. Our analysis indicates that SPOCK2 may be an important gene in the development of PDAC, which should be

confirmed furtherly. CD1D, a member of the CD1 family, is a class of non-polypeptide transmembrane glycoprotein molecules, which is widely expressed in thymocyte B cells, epidermal Langerhans cells, dendritic cells, and intestinal epithelial cells^[40]. With function of antigen presentation similar to MHC I, CD1D can specifically present antigens to NKT cells, make them activate and secrete a variety of cytokines, and directly or indirectly participate in the body's immune response^[41]. Recently, a research about CD1d-binding glycolipid for iNKT-cell-based therapy showed a potent and effective treatment against human breast cancer^[42]. Another clinical phase II study showed that intravenous administration of α -GalCer-pulsed antigen-presenting cells (APCs) prolonged overall survival for patients with advanced or recurrent non-small cell lung cancer^[43]. (α -GalCer—an exogenous glycolipid antigen extracted from sponges—specifically binding to CD1D molecule can activate NKT cells to exert immune effects^[44].) The effect of CD1D-restricted invariant natural killer T (iNKT) cells in PDAC immunotherapy are unclear. However, our analysis suggests that CD1D may have an important role in PDAC. Therefore, we considered CD1D as a promising target for PDAC immunotherapy.

In summary, our findings provide a more comprehensive insight into TME and show a list of prognostic immune associated genes in PDAC. CA9, SPOCK2 and CD1D exhibited significant prognostic potential, and CD1D were significantly related with immune cell biomarkers for PDAC patients, thus indicating the relevance of monitoring and regulating the TME for PDAC prognosis and precision immunotherapies. However, further studies on these genes need to be performed to gain additional understanding of the association between TME and prognosis in PDAC.

Declarations

Ethics approval and consent to participate

Not applicable.

Consent for publication

Not applicable.

Availability of data and materials

Gene expression profile (level 3 data) and clinical information for PDAC patients was collected from the TCGA data portal (<https://tcga-data.nci.nih.gov/tcga/>).

Competing interests

Not applicable.

Funding

This work was supported by National Natural Science Foundation of China (81871927).

Authors' contributions

Zhong Chen and Qian Lu co-designed the study. Qian Lu, Yu Zhang collected the Data and analyzed Identification and Functional enrichment of DEGs. Qian Lu, Weihong Gu constructed the Protein-Protein Interaction (PPI) Network. Qian Lu and Xinrong Ji analyzed Overall Survival and TIMER database. All authors wrote this manuscript together.

Acknowledgements

The author thanks Professor Zhong Chen for reviewing and editing the manuscript.

Reference

- [1] Bray F, Ferlay J, Soerjomataram I, et al. Global cancer statistics 2018: GLOBOCAN estimates of incidence and mortality worldwide for 36 cancers in 185 countries[J]. *CA Cancer J Clin*, 2018, 68(6): 394-424.
- [2] Hidalgo M, Cascinu S, Kleeff J, et al. Addressing the challenges of pancreatic cancer: future directions for improving outcomes[J]. *Pancreatology*, 2015, 15(1): 8-18.
- [3] Siegel R L, Miller K D, Jemal A. Cancer Statistics, 2017[J]. *CA Cancer J Clin*, 2017, 67(1): 7-30.
- [4] Kamisawa T, Wood L D, Itoi T, et al. Pancreatic cancer[J]. *Lancet*, 2016, 388(10039): 73-85.
- [5] Muniraj T, Jamidar P A, Aslanian H R. Pancreatic cancer: a comprehensive review and update[J]. *Dis Mon*, 2013, 59(11): 368-402.
- [6] Chames P, Kerfelec B, Baty D. Therapeutic antibodies for the treatment of pancreatic cancer[J]. *ScientificWorldJournal*, 2010, 10: 1107-1120.
- [7] Le N, Sund M, Vinci A, et al. Prognostic and predictive markers in pancreatic adenocarcinoma[J]. *Dig Liver Dis*, 2016, 48(3): 223-230.
- [8] Coperchini F, Croce L, Marino M, et al. Role of chemokine receptors in thyroid cancer and immunotherapy[J]. *Endocr Relat Cancer*, 2019, 26(8): R465-R478.
- [9] Fang H, Declerck Y A. Targeting the tumor microenvironment: from understanding pathways to effective clinical trials[J]. *Cancer Res*, 2013, 73(16): 4965-4977.
- [10] Roma-Rodrigues C, Mendes R, Baptista P V, et al. Targeting Tumor Microenvironment for Cancer Therapy[J]. *Int J Mol Sci*, 2019, 20(4).
- [11] Wu T, Dai Y. Tumor microenvironment and therapeutic response[J]. *Cancer Lett*, 2017, 387: 61-68.

- [12] Mertins P, Mani D R, Ruggles K V, et al. Proteogenomics connects somatic mutations to signalling in breast cancer[J]. *Nature*, 2016, 534(7605): 55-62.
- [13] Shah N, Wang P, Wongvipat J, et al. Regulation of the glucocorticoid receptor via a BET-dependent enhancer drives antiandrogen resistance in prostate cancer[J]. *Elife*, 2017, 6.
- [14] Guinney J, Dienstmann R, Wang X, et al. The consensus molecular subtypes of colorectal cancer[J]. *Nat Med*, 2015, 21(11): 1350-1356.
- [15] Klemm F, Joyce J A. Microenvironmental regulation of therapeutic response in cancer[J]. *Trends Cell Biol*, 2015, 25(4): 198-213.
- [16] Yoshihara K, Shahmoradgoli M, Martinez E, et al. Inferring tumour purity and stromal and immune cell admixture from expression data[J]. *Nat Commun*, 2013, 4: 2612.
- [17] Ritchie M E, Phipson B, Wu D, et al. limma powers differential expression analyses for RNA-sequencing and microarray studies[J]. *Nucleic Acids Res*, 2015, 43(7): e47.
- [18] Szklarczyk D, Gable A L, Lyon D, et al. STRING v11: protein-protein association networks with increased coverage, supporting functional discovery in genome-wide experimental datasets[J]. *Nucleic Acids Res*, 2019, 47(D1): D607-D613.
- [19] Shannon P, Markiel A, Ozier O, et al. Cytoscape: a software environment for integrated models of biomolecular interaction networks[J]. *Genome Res*, 2003, 13(11): 2498-2504.
- [20] Zhang S, Zhang E, Long J, et al. Immune infiltration in renal cell carcinoma[J]. *Cancer Sci*, 2019, 110(5): 1564-1572.
- [21] Yan H, Qu J, Cao W, et al. Identification of prognostic genes in the acute myeloid leukemia immune microenvironment based on TCGA data analysis[J]. *Cancer Immunol Immunother*, 2019, 68(12): 1971-1978.
- [22] Liao H, Chen W, Dai Y, et al. Expression of Programmed Cell Death-Ligands in Hepatocellular Carcinoma: Correlation With Immune Microenvironment and Survival Outcomes[J]. *Front Oncol*, 2019, 9: 883.
- [23] Merlano M C, Abbona A, Denaro N, et al. Knowing the tumour microenvironment to optimise immunotherapy[J]. *Acta Otorhinolaryngol Ital*, 2019, 39(1): 2-8.
- [24] Xiong Y, Wang K, Zhou H, et al. Profiles of immune infiltration in colorectal cancer and their clinical significant: A gene expression-based study[J]. *Cancer Med*, 2018, 7(9): 4496-4508.
- [25] Heeren A M, Koster B D, Samuels S, et al. High and interrelated rates of PD-L1+CD14+ antigen-presenting cells and regulatory T cells mark the microenvironment of metastatic lymph nodes from

patients with cervical cancer[J]. *Cancer Immunol Res*, 2015, 3(1): 48-58.

[26] Punt S, Corver W E, Van Der Zeeuw S A, et al. Whole-transcriptome analysis of flow-sorted cervical cancer samples reveals that B cell expressed TCL1A is correlated with improved survival[J]. *Oncotarget*, 2015, 6(36): 38681-38694.

[27] Eo W K, Kwon S, Koh S B, et al. The Lymphocyte-Monocyte Ratio Predicts Patient Survival and Aggressiveness of Endometrial Cancer[J]. *J Cancer*, 2016, 7(5): 538-545.

[28] Protti M P, De Monte L, Di Lullo G. Tumor antigen-specific CD4+ T cells in cancer immunity: from antigen identification to tumor prognosis and development of therapeutic strategies[J]. *Tissue Antigens*, 2014, 83(4): 237-246.

[29] Adams O J, Stanczak M A, Von Gunten S, et al. Targeting sialic acid-Siglec interactions to reverse immune suppression in cancer[J]. *Glycobiology*, 2018, 28(9): 640-647.

[30] McDonald P C, Chafe S C, Brown W S, et al. Regulation of pH by Carbonic Anhydrase 9 Mediates Survival of Pancreatic Cancer Cells With Activated KRAS in Response to Hypoxia[J]. *Gastroenterology*, 2019, 157(3): 823-837.

[31] Michaud D, Mirlekar B, Bischoff S, et al. Pancreatic cancer-associated inflammation drives dynamic regulation of p35 and Ebi3[J]. *Cytokine*, 2020, 125: 154817.

[32] Supuran C T, Winum J Y. Carbonic anhydrase IX inhibitors in cancer therapy: an update[J]. *Future Med Chem*, 2015, 7(11): 1407-1414.

[33] Vitoratou D I, Tolia M, Liakos P, et al. Clinical value of significance of Hypoxia Inducible Factor-1alpha, Glucose Transporter-1 and Carbonic Anhydrase IX in rectal cancer after preoperative chemoradiotherapy[J]. *J BUON*, 2019, 24(2): 456-463.

[34] Giatromanolaki A, Harris A L, Banham A H, et al. Carbonic anhydrase 9 (CA9) expression in non-small-cell lung cancer: correlation with regulatory FOXP3+T-cell tumour stroma infiltration[J]. *Br J Cancer*, 2020.

[35] Iikuni S, Ono M, Watanabe H, et al. Cancer radiotheranostics targeting carbonic anhydrase-IX with (111)In- and (90)Y-labeled ureidosulfonamide scaffold for SPECT imaging and radionuclide-based therapy[J]. *Theranostics*, 2018, 8(11): 2992-3006.

[36] Lou W, Ding B, Zhong G, et al. Dysregulation of pseudogene/lncRNA-hsa-miR-363-3p-SPOCK2 pathway fuels stage progression of ovarian cancer[J]. *Aging (Albany NY)*, 2019, 11(23): 11416-11439.

[37] Sambuudash O, Kim H S, Cho M Y. Lack of Aberrant Methylation in an Adjacent Area of Left-Sided Colorectal Cancer[J]. *Yonsei Med J*, 2017, 58(4): 749-755.

- [38] Ren F, Wang D B, Li T. [Epigenetic inactivation of SPOCK2 in the malignant transformation of ovarian endometriosis][J]. Zhonghua Fu Chan Ke Za Zhi, 2011, 46(11): 822-825.
- [39] Ren F, Wang D, Wang Y, et al. SPOCK2 Affects the Biological Behavior of Endometrial Cancer Cells by Regulation of MT1-MMP and MMP2[J]. Reprod Sci, 2019: 1933719119834341.
- [40] King L A, Lameris R, De Gruijl T D, et al. CD1d-Invariant Natural Killer T Cell-Based Cancer Immunotherapy: alpha-Galactosylceramide and Beyond[J]. Front Immunol, 2018, 9: 1519.
- [41] Melo A M, Conroy M J, Foley E K, et al. CD1d expression and invariant natural killer T-cell numbers are reduced in patients with upper gastrointestinal cancers and are further impaired by commonly used chemotherapies[J]. Cancer Immunol Immunother, 2020.
- [42] Seki T, Liu J, Brutkiewicz R R, et al. A Potent CD1d-binding Glycolipid for iNKT-Cell-based Therapy Against Human Breast Cancer[J]. Anticancer Res, 2019, 39(2): 549-555.
- [43] Toyoda T, Kamata T, Tanaka K, et al. Phase II study of alpha-galactosylceramide-pulsed antigen-presenting cells in patients with advanced or recurrent non-small cell lung cancer[J]. J Immunother Cancer, 2020, 8(1).
- [44] Kanamori T, Numata T, Kuwabara S, et al. Photo effect on the CD1d-binding ability of azobenzene-attached analogues of alpha-GalCer[J]. Bioorg Med Chem Lett, 2020, 30(5): 126960.

Tables

Table 1. GO and KEGG pathway enrichment analysis of DEGs with immune and stromal score in PDAC.

Term	Description	PValue	Count in gene set
GO:0046651	lymphocyte proliferation	2.56616E-15	19
GO:0032943	mononuclear cell proliferation	2.97786E-15	19
GO:0050670	regulation of lymphocyte proliferation	9.59315E-15	17
GO:0001772	immunological synapse	4.35256E-06	5
GO:0042101	T cell receptor complex	0.000187906	3
GO:0101003	ficolin-1-rich granule membrane	0.000559228	4
GO:0042609	CD4 receptor binding	7.22954E-06	3
GO:0023023	MHC protein complex binding	7.18771E-06	4
GO:0033691	sialic acid binding	3.08218E-05	3
KEGG:03320	PPAR signaling pathway	0.00152816	4
KEGG:04640	Hematopoietic cell lineage	1.33E-08	9
KEGG:04657	IL-17 signaling pathway	0.000391126	5

Table 2. Univariate and multivariate Cox logistic regression analysis of overall survival in TCGA cohort.

	Univariate analysis				Multivariate analysis (adjusted for age)			
	HR	<i>P</i> > z	95% CI		HR	<i>P</i> > z	95% CI	
EBI3expression High vs low	0.593	0.014	0.391	0.901	0.852	0.839	0.183	3.975
WDFY4expression High vs low	0.747	0.180	0.488	1.143	1.509	0.498	0.459	4.965
P2RY8expression High vs low	0.622	0.025	0.410	0.943	1.895	0.320	0.538	6.670
CA9expression High vs low	1.754	0.010	1.145	2.687	2.751	0.008	1.307	5.794
PLA2G2Dexpression High vs low	0.692	0.080	0.459	1.044	1.194	0.746	0.408	3.489
CD36expression High vs low	0.561	0.007	0.369	0.852	0.624	0.432	0.193	2.022
SPOCK2expression High vs low	0.621	0.025	0.410	0.941	3.310	0.016	1.251	8.758
CD1Dexpression High vs low	0.642	0.045	0.416	0.991	0.212	0.034	0.050	0.893
CCL22expression High vs low	0.629	0.030	0.414	0.956	0.625	0.267	0.272	1.434
T 1 vs 2 and 3 vs 4	1.636	0.025	1.065	2.513	0.372	0.069	0.128	1.080
N 0 vs 1	2.152	0.004	1.281	3.616	2.849	0.029	1.116	7.274
M 0 vs 1	0.756	0.701	2.466	5.124	0.784	0.769	0.155	3.960

Figures

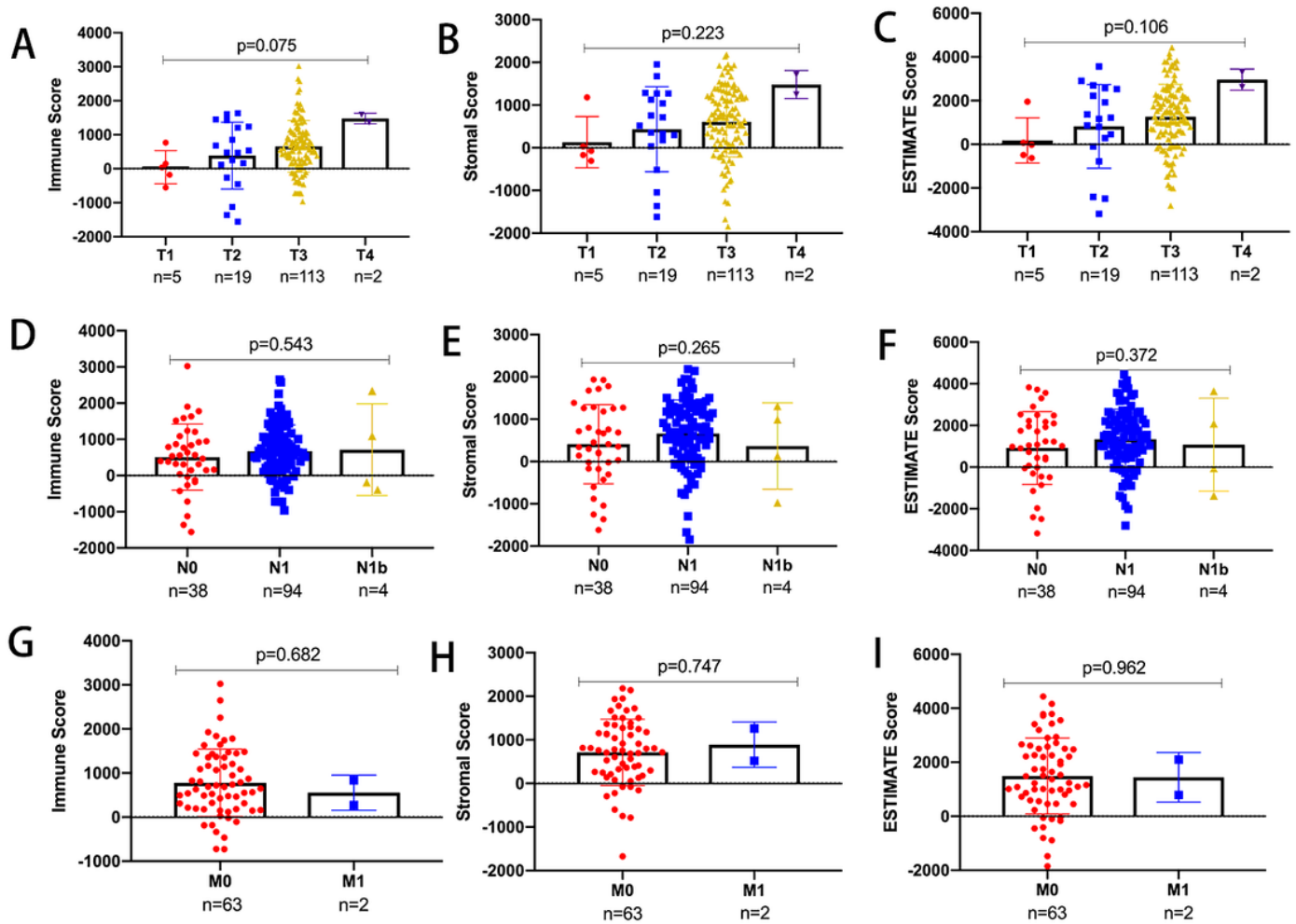


Figure 1

Immune, stromal, and ESTIMATE scores were not correlated with T stage, N stage, or M stage. Distribution of immune scores plotted against T stage (A), N stage (D), and M stage (G). Distribution of stromal scores plotted against T stage (B), N stage (E), and M stage (H). Distribution of ESTIMATE scores plotted against T stage (C), N stage (F), and M stage (I)

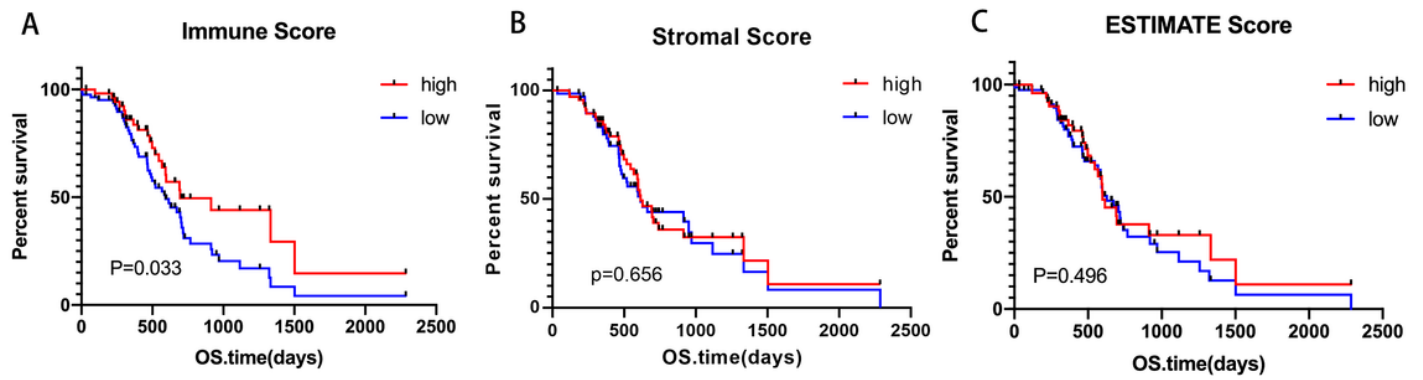


Figure 2

Association of immune, stromal, and ESTIMATE scores with overall survival. (A) Elevated immune scores correlated with a better prognosis. (B) Stromal scores were not associated with overall survival. (C) ESTIMATE scores were not associated with overall survival.

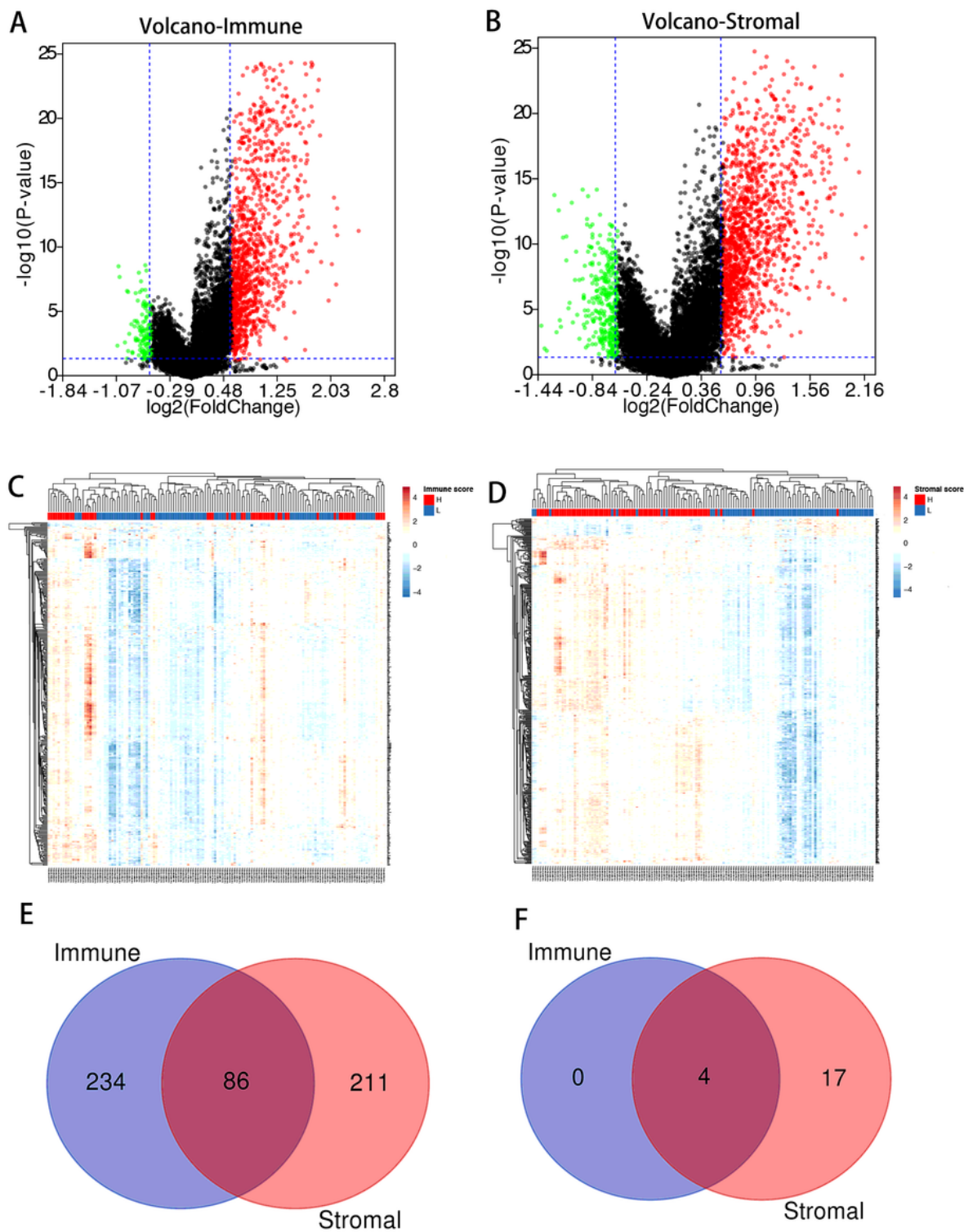
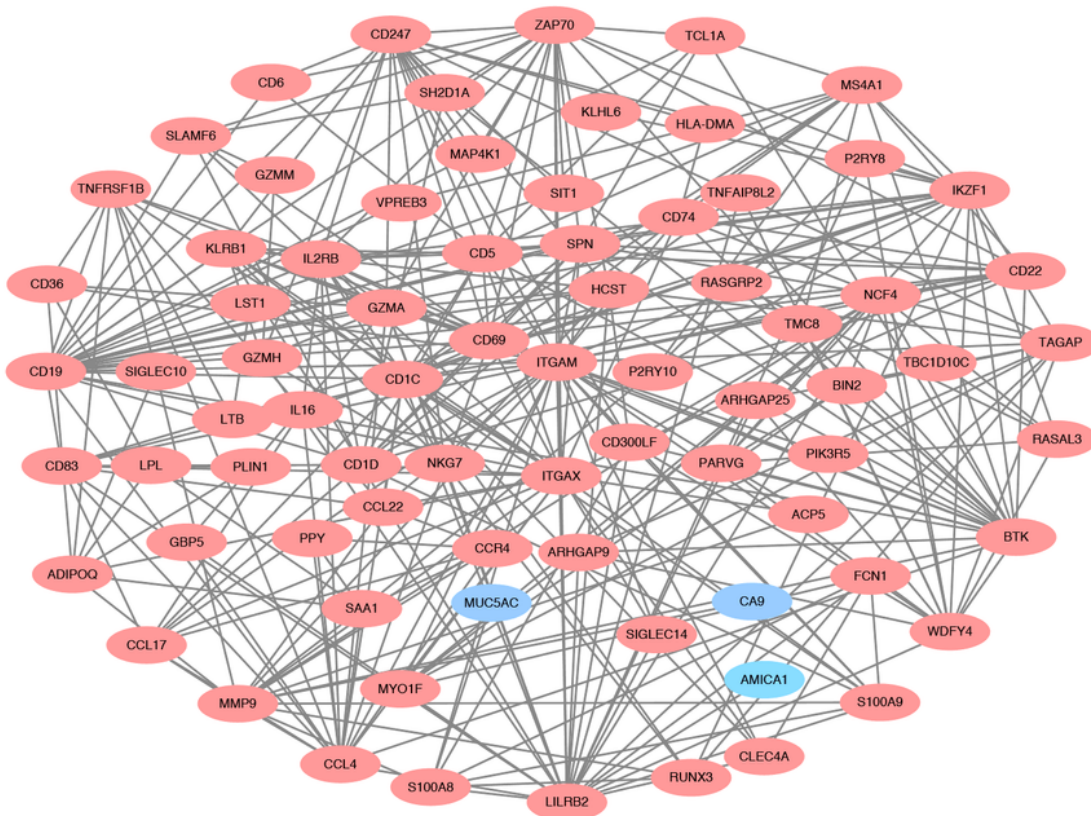


Figure 3

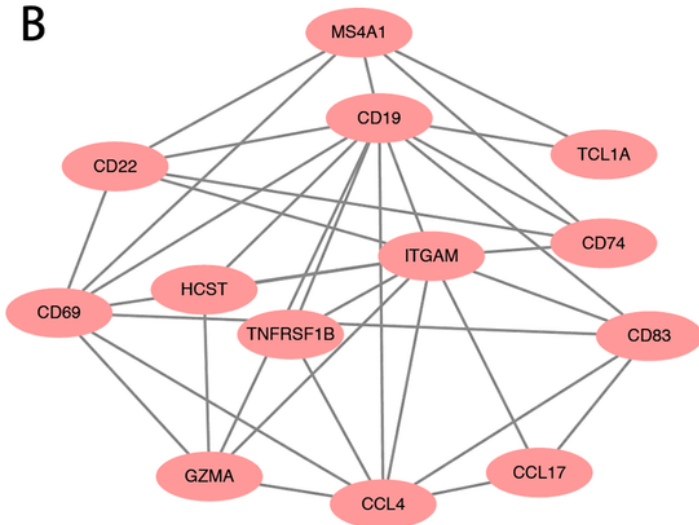
Comparison of gene expression profile with immune scores and stromal scores in PDAC (A) Volcano maps show the distribution of DEGs based on immune scores. (B) Volcano maps show the distribution of DEGs based on stromal scores. Red and green dots represent high and low expressed genes, respectively. (C) Heatmaps of DEGs of immune scores. (D) Heatmaps of DEGs of stromal scores. (E) Venn diagrams

showing the number of commonly upregulated DEGs in stromal and immune. (F) Venn diagrams showing the number of commonly downregulated DEGs in stromal and immune.

A



B



C

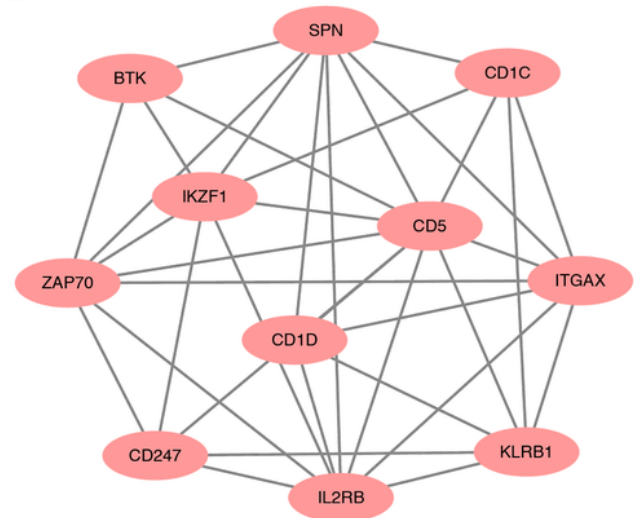


Figure 4

PPI network and the most significant module of DEGs. (A) The PPI network of DEGs was constructed using Cytoscape. (B, C) The top two significant module was obtained from PPI network using MCODE. Upregulated genes are marked in light red; downregulated genes are marked in light blue.

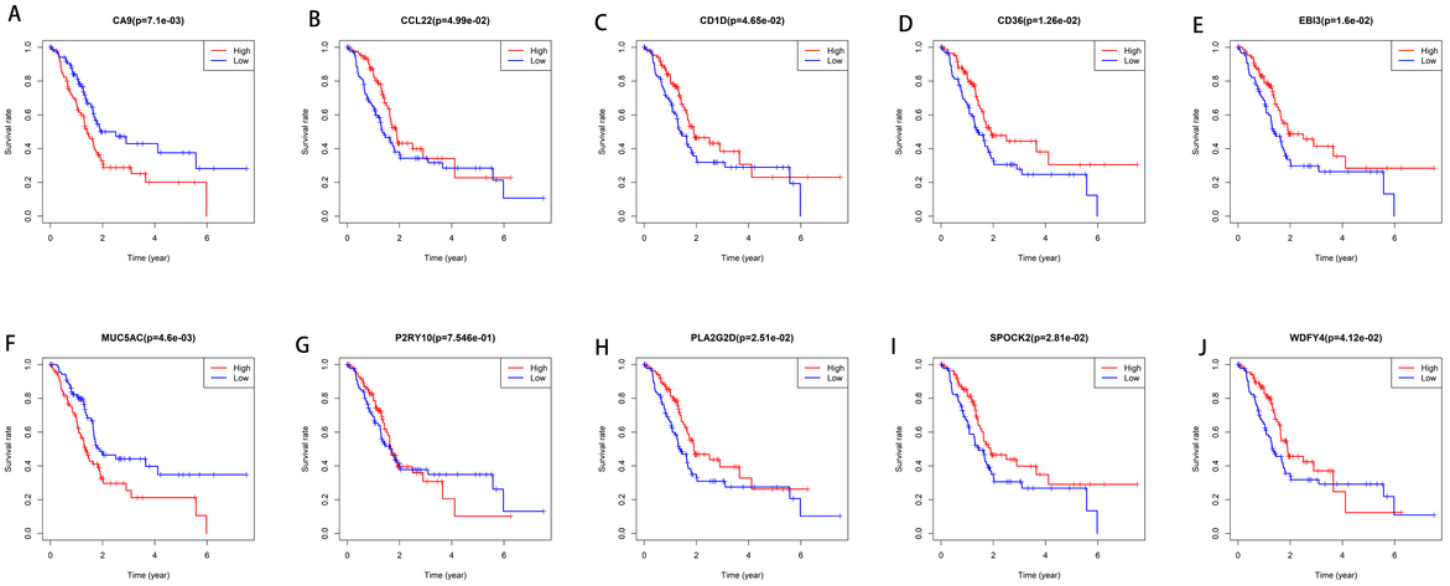


Figure 5

Correlation of expression of individual DEGs with overall survival in TCGA. KM survival curves were plotted for selecting DEGs with prognostic value by comparison of groups of high (red line) and low (blue line) gene expression.

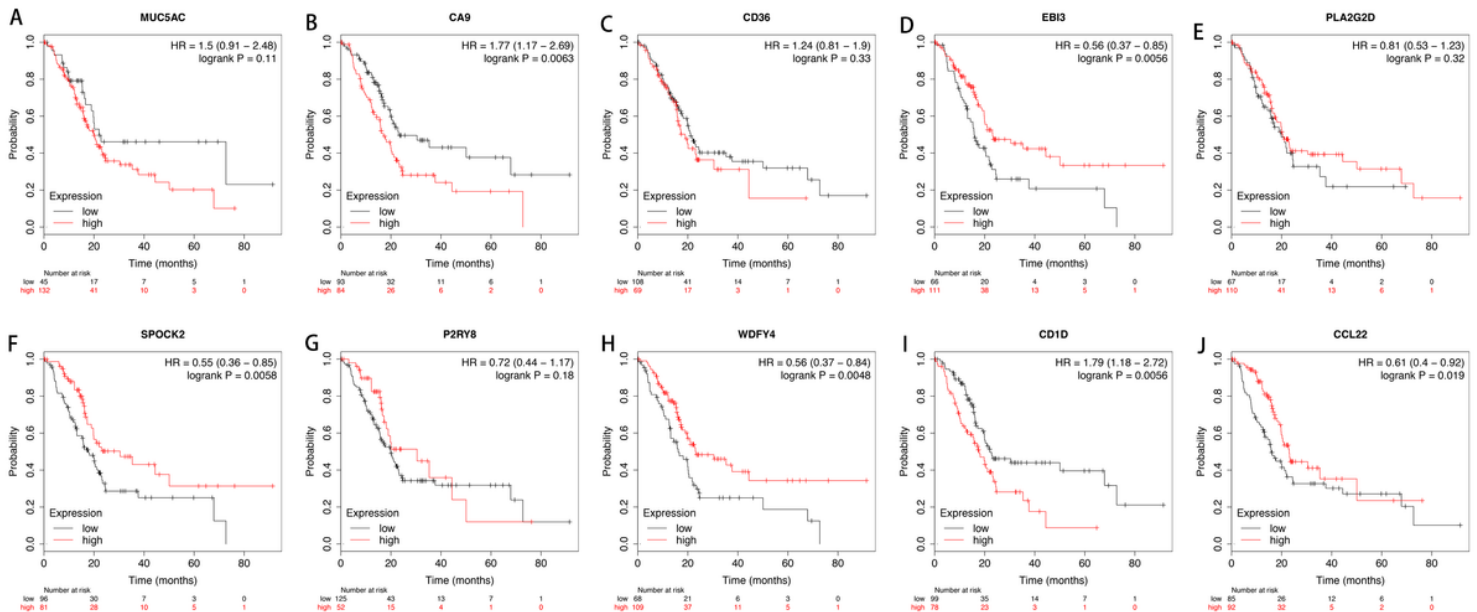


Figure 6

Validation of correlation of DEGs extracted from the TCGA database with overall survival by Kaplan-Meier plotter online analysis tool. KM survival curves were plotted for selecting DEGs with prognostic value by comparison of groups of high (red line) and low (black line) gene expression.

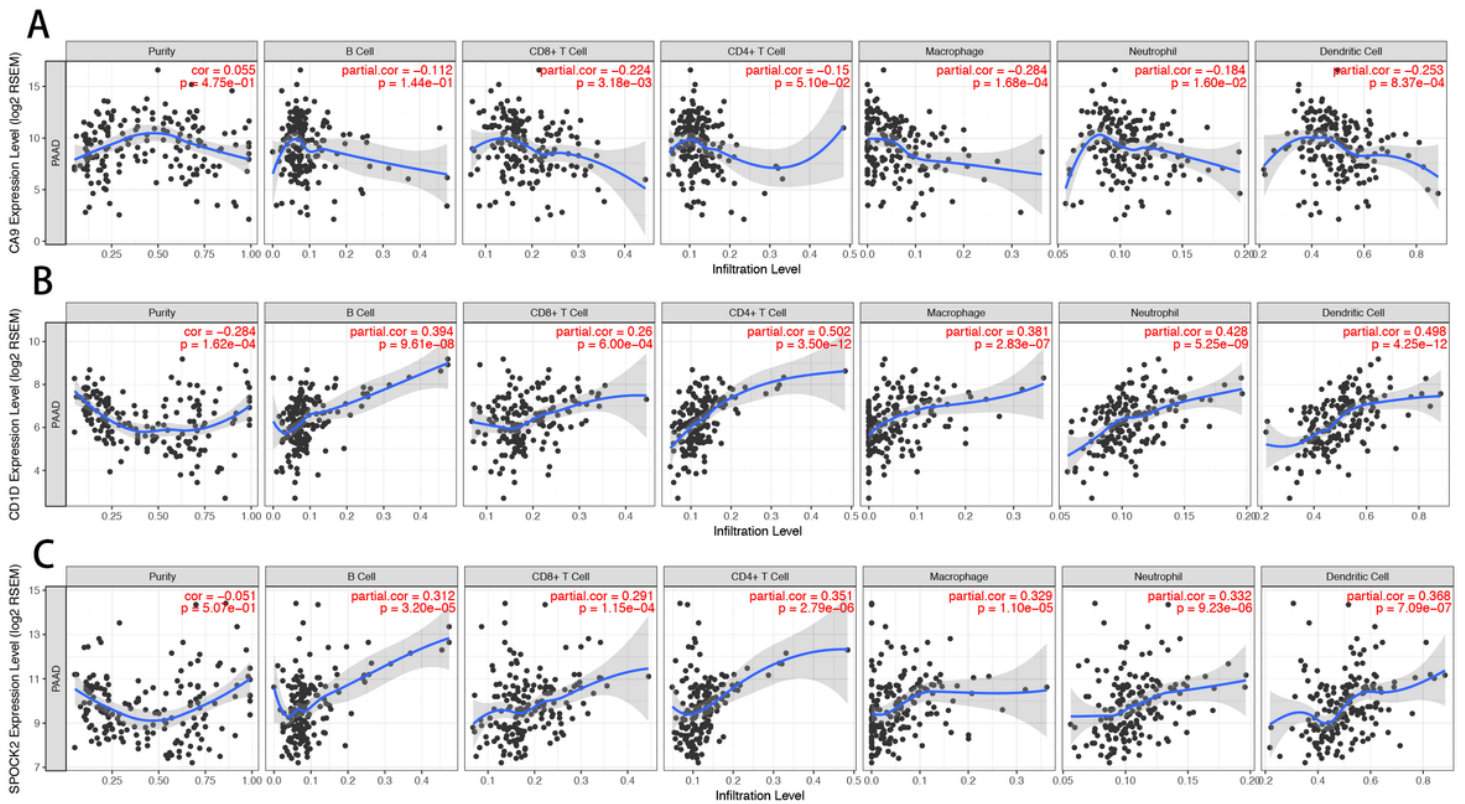


Figure 7

Immune infiltration of CA9, SPOCK2 and CD1D. After identifying prognostic value of CA9, CD1D and SPOCK2, we performed correlation analysis between CA9, CD1D and SPOCK2 and immune infiltration level for PDAC. Scatter plots were generated with partial Spearman's correlation and statistical significance. (A) CA9 expression has a significant positive correlation with infiltrating levels of CD8+ T cell, macrophage, neutrophil, and dendritic cells in PDAC. (B) SPOCK2 expression has a significant positive correlation with infiltrating levels of B cell, CD8+ T cell, CD4+ T cell, macrophage, neutrophil, and dendritic cells in PDAC. (C) CD1D expression has a significant positive correlation with infiltrating levels of purity, B cell, CD8+ T cell, CD4+ T cell, macrophage, neutrophil, and dendritic cells in PDAC.

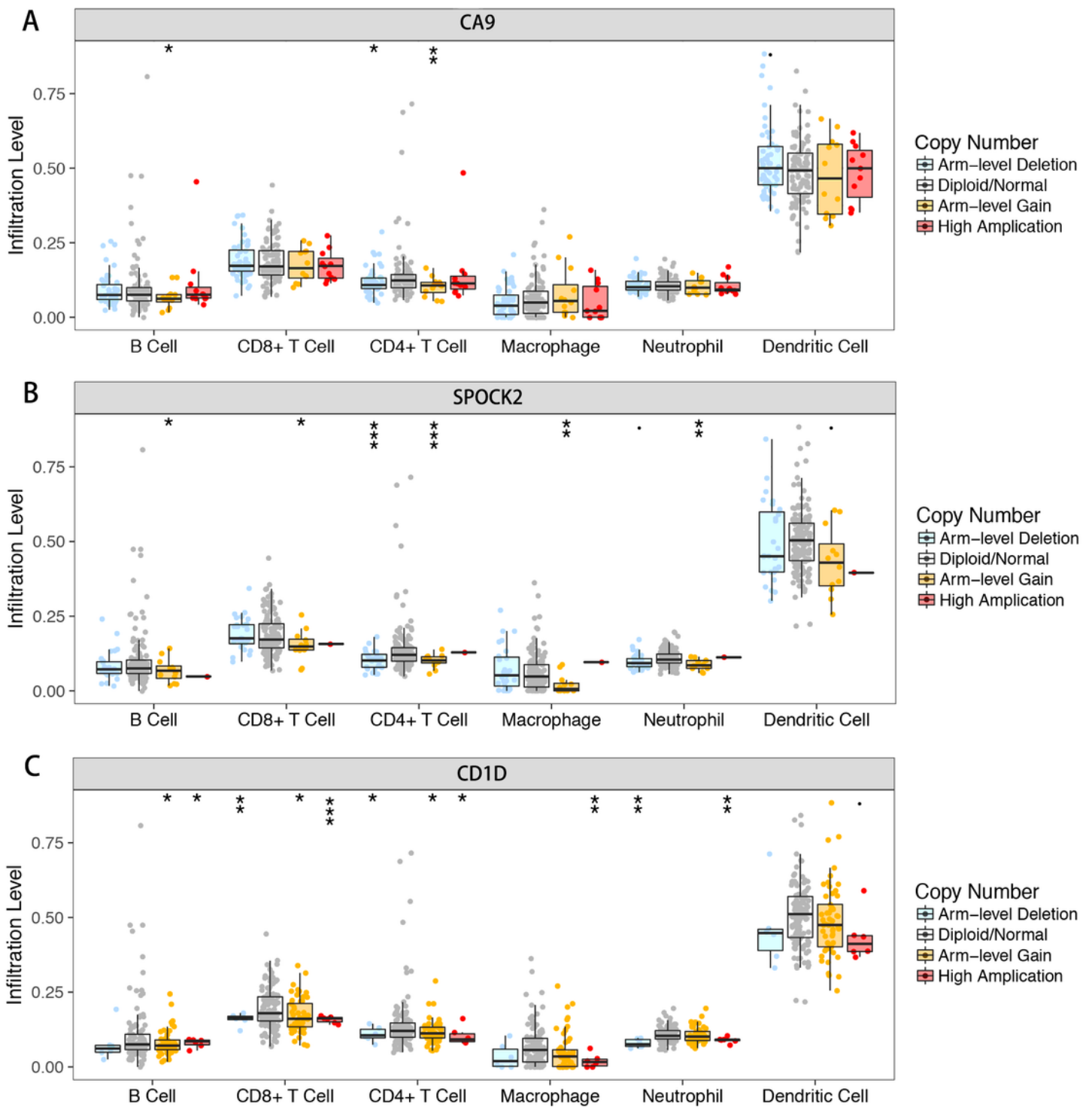


Figure 8

The association of SCNAs of CA9, SPOCK2 and CD1D with immune infiltration in PDAC. In the genomic datasets, SCNAs of CA9, SPOCK2 and CD1D were divided into into four levels, including arm-level deletion, diploid/normal, arm-level gain, and high amplification. The infiltration of six immune cell types, including B cell, CD 8+T cell, CD4+T cell, macrophage cell, neutrophil cell and dendritic cell, was analyzed in PDAC. (A) Enrichment of B cell, CD4+T cell displayed significant downregulation in PDAC with

particular SCNA of CA9. (B) Enrichment of B cell, CD 8+T cell, CD4+T cell, macrophage cell and neutrophil cell displayed significant downregulation in PDAC with particular SCNA of SPOCK2. (C) Enrichment of B cell, CD 8+T cell, CD4+T cell, macrophage cell and neutrophil cell displayed significant downregulation in PDAC with particular SCNA of CD1D.